ELSEVIER

Earth and Planetary Science Letters 198 (2002) 225–243

EPSL

www.elsevier.com/locate/epsl

The duration of ordinary chondrite metamorphism inferred from tungsten microdistribution in metal

Munir Humayun *, Andrew J. Campbell

Department of the Geophysical Sciences, The University of Chicago, 5734 S. Ellis Avenue, Chicago, IL 60637, USA

Received 10 October 2001; received in revised form 11 January 2002; accepted 30 January 2002

Abstract

Precise ratios of W and Re relative to Ir determined by laser ablation ICP-MS reveal that matrix metal in equilibrated ordinary chondrites (EOC) exhibits a correlated variation of these ratios. In unequilibrated ordinary chondrites (UOC), the W/Ir ratio varies by over two orders of magnitude (W/Ir = 0.003–0.6), and shows no correlation with any other siderophile element. Most matrix metal in UOC is depleted in W relative to metal in EOC. Thus, W must enter metal during metamorphism. The correlation between W/Ir and Re/Ir is evident in type 4 chondrites. This implies that the abundance (and isotopic composition) of W is set in ordinary chondrite metal by petrologic type 4, and that the reductant must be exhausted to limit further isotopic exchange, as indicated by the ^{182}Hf–^{182}W ages of ordinary chondrite metal [Lee and Halliday, Science 274 (1996) 1876–1879]. This offers a means of dating the onset of metamorphic heating of OC parent bodies. A discrepancy in ages between ^{182}Hf–^{182}W [Lee and Halliday, Science 274 (1996) 1876–1879] and ^{207}Pb–^{206}Pb [Göpel et al., Earth Planet. Sci. Lett. 121 (1994) 153–171] (or ^{129}I-^{129}Xe [Brazzle et al., Geochim. Cosmochim. Acta 63 (1999) 739–760]) dating is real, and measures the interval of metamorphism: the time difference between reduction of W during the onset of heating and isotopic closure of Pb (or Xe) by cooling, e.g., ΔT_m = 2–12 Myr for H chondrites. The ^{187}Re–^{187}Os and ^{182}Hf–^{182}W ages are set by the same process, metamorphic equilibration, establishing an important link between an absolute chronometer ($t_{1/2}$[^{187}Re] = 41.6 billion years) and a short-lived radioisotope system ($t_{1/2}$[^{182}Hf] = 9 Myr).

Keywords: ordinary chondrites; metals; siderophile elements; tungsten; platinum group

1. Introduction

One of the major goals of cosmochronology is to combine the timescales derived from long-lived radionuclides (e.g., ^{147}Sm–^{143}Nd, ^{187}Re–^{187}Os, U–Th–Pb) with those derived from short-lived radionuclides (e.g., ^{26}Al–^{26}Mg, ^{107}Pd–^{107}Ag, ^{146}Sm–^{142}Nd, ^{182}Hf-^{182}W) to yield a more detailed understanding of the sequence of early solar system processes such as condensation, accretion, core formation and magmatic differentiation [1–5]. Reading this record of early solar system history is complicated by the distinct geochemical properties of these parent–daughter systems (e.g., lithophile or siderophile, refractory or volatile) and by a relatively limited understanding of their behav-

* Corresponding author. Tel.: +1-773-834-1337; Fax: +1-773-702-9505.

E-mail address: hum8@midway.uchicago.edu (M. Humayun).

0012-821X/02/$ – see front matter
PII: S0012-821X(02)00500-9

ior during subsequent metamorphic (or shock) processes that may disturb or reset these chronometers [2,6].

The ordinary chondrites (OC) constitute the largest class of meteorites, and exhibit the entire range of metamorphic conditions from type 3 (unequilibrated) to type 6 (highly equilibrated). Ordinary chondrites have abundant metal and exhibit metal–silicate fractionation, defining the major subgroups (H, L, LL). Göpel et al. [7] determined the U–Pb ages of phosphates formed during metamorphism by oxidation of P from metal and obtained a correlation between ^{207}Pb–^{206}Pb closure age and metamorphic grade for H chondrites. They obtained a spread in phosphate ^{207}Pb–^{206}Pb ages of almost 60 Myr, with the most metamorphosed chondrites giving the youngest ages. The observed age spectrum of OC is in the right range for the application of the new ^{182}Hf–^{182}W chronometer ($t_{1/2}$ = 9 Myr [4]). Lee and Halliday [4] determined that ^{182}W/^{184}W ratios for OC metal exhibited little variation with metamorphic grade, and were similar to those in iron meteorites, i.e., solar system initial W isotopic compositions. Lee and Halliday [4] concluded that the ^{207}Pb–^{206}Pb ages of [7] had been 'disturbed', and that the ^{182}Hf–^{182}W ages provided more accurate measures of the timing of metamorphism relative to the formation of the solar system. Thus, these two chronometer pairs yielded apparently inconsistent results for the timing of OC metamorphism. A recent study of the ^{129}I–^{129}Xe system, based on the decay of ^{129}I ($t_{1/2}$ = 15.7 Myr), in phosphates and feldspars from OC [5] confirmed the time differences obtained from the ^{207}Pb–^{206}Pb system [7]. The discrepancy between time differences obtained from OC phosphates and feldspars by ^{207}Pb–^{206}Pb and ^{129}I–^{129}Xe and those obtained from OC metal by ^{182}Hf–^{182}W have not been explained.

Metamorphic processes, terrestrial or extraterrestrial, reset radioactive chronometers by diffusive equilibration at peak temperatures. During cooling, various radioactive parent-bearing mineral phases reach their closure temperatures and begin recording the passage of time [7–9]. Thus, metamorphic 'ages' are measures of time elapsed since cooling of a rock or mineral through its closure temperature. No chronometer has yet been described that can determine the timing of the initiation of metamorphism. Wasserburg et al. [10] inferred a 'timescale of metamorphism' of 74 Myr for the H chondrites, using differences between the initial ^{87}Sr/^{86}Sr of phosphate from Guareña (H6) and that of BABI evolving in a 'chondritic Rb/Sr' system. Such an interval of metamorphism is similar to the ~60 Myr inferred by ^{207}Pb–^{206}Pb dating of chondritic phosphates from unequilibrated and equilibrated ordinary chondrites [7]. Both these methods determine an interval of metamorphism from the difference in closure times of a single chronometer applied to a set of chondrites.

Since metal is abundant in OC, the siderophile elements should be largely present in the metal phase, at least in equilibrated ordinary chondrites. Detailed studies of the distribution of siderophile elements in bulk EOC metal [11–17] showed that siderophiles were not present in chondritic proportions, for reasons that were not clear. Particularly, Re/Ir ratios were noted to be higher in metal than in bulk chondrites [12,17]. Chen et al. [18] applied the ^{187}Re–^{187}Os chronometer to metal in EOC and found that Re/Os ratios were distinctly higher in metal than in bulk chondrites, in some cases, by a factor of two. Chen et al. [18] observed that such a large fractionation of Re/Os ratio was only known from magmatic iron meteorites. They proposed a model for chondrite formation involving fractional crystallization in molten planetesimals, followed by impact disruption, and reassembly of molten silicate (chondrules) and metal droplets. The platinum group element (PGE) fractionation was postulated to occur in such a magmatic process. Previous attempts at characterizing the trace element microdistribution of chondritic metal succeeded in determining the abundances of Os, Ir, Pt and Au by ion microprobe techniques [19]. Due to low ion yields, the analysis of Re and W has not been possible using the methods of [19,20].

Humayun and Campbell [21] determined the microdistribution of the refractory siderophiles Re, Os, Ir and Pt, in EOC metal by laser ablation inductively coupled plasma mass spectrometry (LA-ICP-MS), and showed that Os and Ir were

deficient in EOC metal relative to Fe, while Re/Fe ratios were often chondritic. They further showed that Ir/Os–Re/Os ratios in EOC metal were inconsistent with fractional crystallization in magmatic iron systems, and proposed that the observed Re/Os fractionations were caused by redox processes during metamorphism. The experimental design of [21] was optimized for precise Re/Os determinations, and W had not been included in the list of elements determined. Tungsten is a refractory siderophile element, that oxidizes more readily than Re and the PGEs, and is an essential element to study redox-related processes in OC metal. Here, we report precise W/Ir, Re/Ir, Os/Ir and Pt/Ir ratios determined on individual metal grains from Weston (H4), Allegan (H5), Kernouve (H6), Soko-Banja (LL4) and Alfianello (L6) (EOC), and from Tieschitz (H3.4–3.6), Mezö-Madaras (L3.7), and Parnallee (LL3.6) (UOC). These data are used to infer the behavior of these siderophile elements during metamorphism, with implications for the ^{182}Hf–^{182}W and ^{187}Re–^{187}Os chronometers. Preliminary results were reported by Humayun and Campbell [22,23]. In this paper, we reconcile the apparently inconsistent results from the ^{207}Pb–^{206}Pb and ^{182}Hf–^{182}W chronometers, and provide a measure of the interval of metamorphism on the OC parent body. The implications of the present study to models of the Re/Os evolution of the Earth's core, which have relied on H5 chondrite metal [55–57] as a compositional analog, are presented.

2. Analytical techniques

Prior to laser ablation, thin sections and/or polished slabs of Tieschitz (H3.4–3.6), Weston (H4), Allegan (H5), Kernouve (H6), Mezö-Madaras (L3.7), Alfianello (L6), Parnallee (LL3.6), and Soko-Banja (LL4), were mapped by scanning electron microscopy, and matrix metal grains were selected for trace element microanalysis by LA-ICP-MS. All eight chondrites studied were observed falls. Assignment of metamorphic type for UOC follows [24,25]. Data were acquired using a CETAC Technologies LSX-200, 266 nm UV laser ablation system coupled to a magnetic sector, high resolution ICP-MS, the Finnigan Element™. The analytical procedure of [21] was modified to include W. During the normal analytical procedure [26,27], which collects peaks over a mass range from ^{7}Li to ^{197}Au, the Element™ has a duty cycle (fraction of time on peaks) of 50%. The low duty cycle is due to the large number of magnet jumps required for this mass range. To improve the duty cycle to 95% for interelement ratio measurements, each point was

Table 1
Abundances of Co, Ni and Ir, and ratios of W, Re, Os, Pt, and Au to Ir for metal from the IIA iron meteorite, Filomena (North Chile, USNM 1334) determined by LA-ICP-MS

Sample	Co (wt%)	Ni (wt%)	Ir (ppm)	W/Ir	Re/Ir	Os/Ir	Pt/Ir	Au/Ir
Filomena IIA								
F-3	0.50	6.32	3.47	0.73	0.062	0.32	6.19	0.19
F-5	0.45	5.27	3.19	0.69	0.081	0.36	6.09	0.17
F-7	0.48	5.36	3.58	0.76	0.050	0.32	6.01	0.18
F-9	0.40	–	2.93	0.79	0.075	0.35	6.14	0.18
F-11	0.48	6.51	3.86	0.83	0.080	0.34	6.28	0.19
F-49	0.50	5.45	4.67	0.70	0.065	0.38	6.49	0.16
F-51	0.49	5.88	2.91	0.63	0.053	0.32	5.88	0.19
F-53	0.35	4.51	3.85	0.80	0.052	0.35	6.32	0.20
F-55	0.40	3.90	2.82	0.81	0.068	0.35	6.94	0.20
Average	0.45	5.40	3.48	0.75	0.065	0.34	6.26	0.18
1σ relative S.D. (%)	12	16	17	9	18	6	5	7
NAA [59,60]	0.454	5.65	3.37	0.76	0.069	0.338	6.14	0.18

Neutron activation analyses of [59], except Os from [60], are shown for comparison.

Table 2
Abundances of Co, Ni and Ir, and ratios of W, Re, Os, and Pt to Ir for H chondrite metal determined by LA-ICP-MS

Sample	Co (wt%)	Ni (wt%)	Ir (ppm)	W/Ir	Re/Ir	Os/Ir	Pt/Ir
Tieschitz (H3.4–3.6)							
Kamacite:							
#16	0.55	4.69	2.17	0.31	0.11	0.96	1.73
#17	0.58	5.18	2.77	0.33	0.09	0.94	1.64
#18	*0.76*	*5.66*	*0.01*	*0.85*	–	–	*2.51*
#19	0.87	6.08	7.02	0.02	0.10	1.02	2.20
#20	0.56	7.51	3.61	0.02	0.14	1.14	1.78
#21	0.70	4.04	1.66	1.21	0.07	0.98	1.49
#22	0.70	4.75	1.21	0.004	0.11	0.93	1.99
#24	0.62	3.62	6.33	0.02	0.09	0.85	1.67
Taenite:							
#23	*0.11*	*45.3*	*0.01*	*2.57*	–	–	*34.8*
#25	0.27	38.3	0.83	0.12	0.16	2.00	3.91
#26			0.84	0.03	0.16	1.85	2.50
#27			1.76	0.12	0.07	0.89	1.27
#28			0.54	0.18	0.19	1.59	3.38
#29			4.17	0.012	0.11	1.03	1.79
Bulk metal [12,14]	0.62	11.8	5.3	0.041	0.12	1.25	3.42
Weston (H4)							
Kamacite:							
#16	0.57	6.18	3.70	0.063	0.12	0.94	2.49
#17	0.46	6.86	12.5	0.54	0.07	1.08	1.67
#18	0.36	5.51	2.99	0.09	0.14	0.89	2.18
#19	0.46	6.28	8.01	0.21	0.08	0.57	5.40
#20	0.45	6.67	16.6	0.15	0.03	0.26	3.67
#21	0.51	7.51	3.66	0.15	0.04	0.33	2.54
#22	0.39	8.03	3.93	0.09	0.04	0.40	1.07
#23	0.49	7.21	15.4	0.27	0.07	0.74	2.39
#25	0.43	10.3	5.22	0.38	0.12	0.89	2.20
#26	0.43	10.1	9.02	0.26	0.10	1.09	2.15
Taenite:							
#13	0.13	20.7	5.41	0.19	0.27	1.16	3.10
#14	0.44	20.6	2.13	10.84	–	2.06	18.15
#24	0.17	21.9	13.0	0.08	0.11	0.93	2.41
Allegan (H5)							
Kamacite:							
#42	0.46	7.07	1.48	0.45	0.19	1.27	2.75
#43	0.49	7.73	1.50	0.53	0.17	1.25	2.55
#48	0.47	6.79	1.45	0.61	0.13	1.28	3.26
#51	0.40	7.18	1.61	0.62	0.14	1.12	2.19
#52	0.44	5.88	1.77	0.47	0.12	1.21	2.37
#53	0.44	6.49	1.15	0.62	0.19	0.95	2.59
#54	0.50	6.12	1.64	0.43	0.11	1.20	2.41
Taenite:							
#44	*0.16*	*28.9*	*0.43*	*1.75*	*1.99*	*1.93*	*14.3*
#45	0.16	27.6	4.56	0.18	0.14	1.80	1.98
#46	0.16	32.0	8.56	0.10	0.13	1.18	2.91
#47	0.13	29.2	4.31	0.19	0.24	0.91	2.99
#49	0.16	24.9	2.32	0.30	0.29	1.16	3.25
#50	0.15	29.5	5.84	0.15	0.18	1.04	1.98
Bulk metal [12,14]	0.49	8.2	3.4	0.25	0.10	1.06	2.21

Table 2 *(continued)*
Abundances of Co, Ni and Ir, and ratios of W, Re, Os, and Pt to Ir for H chondrite metal determined by LA-ICP-MS

Sample	Co (wt%)	Ni (wt%)	Ir (ppm)	W/Ir	Re/Ir	Os/Ir	Pt/Ir
Kernouve (H6)							
Kamacite:							
#15	0.55	6.44	3.02	0.42	0.15	1.13	2.33
#17	0.58	7.26	3.50	0.32	0.14	1.07	2.14
#23	0.46	6.28	6.81	0.48	0.14	0.96	2.07
#25	0.54	7.09	2.04	0.54	0.21	1.08	2.58
#27	0.51	6.87	2.89	0.35	0.11	1.03	2.06
#31	0.48	6.70	3.03	0.57	0.17	1.17	2.33
#35	0.44	6.08	4.17	1.24	0.13	1.09	2.04
#37	0.51	5.80	1.99	0.42	0.11	1.07	1.91
#39	0.50	7.48	2.82	0.41	0.14	1.09	1.92
#41	0.51	6.59	2.36	0.34	0.13	1.04	1.78
Taenite:							
#19	0.20	26.9	3.41	0.26	0.15	0.96	2.45
#21	0.15	26.5	3.84	0.23	0.15	1.06	2.49
Bulk metal [12,14]	0.48	9.4	4.5	0.23	0.10	1.02	2.18
Average H3 metal [17]	0.42	10.4	3.66	0.128	0.102	1.098	2.70
Average H4–6 metal [17]	0.467	9.05	3.08	0.253	0.112	1.003	2.247
Bulk H chondrites[a]	0.083	1.63	0.791	0.210	0.092	1.072	1.84

[a] Bulk H chondrite abundances from [30], except Os/Ir ratio and Co, Ni and Ir abundances from [61].
Metal grains with extremely low Ir abundances are italicized. Sources of meteorite specimens: Tieschitz (L3443) from the Naturhistorisches Museum, Vienna, Austria; Weston (Me 1836) and Allegan (Me 1432) from the Field Museum of Natural History, Chicago, IL, USA; Kernouve (USNM 359) from the Smithsonian Institution, Washington, DC, USA.

analyzed twice. The magnet was settled at m/e = 182, and a 20–50 pulse laser burst was used to measure the isotopes ^{182}W, ^{185}Re, ^{190}Os, ^{193}Ir, and ^{195}Pt using rapid electric scanning (1 ms switching time) by varying the accelerating voltage (8.5 kV) to acquire these peaks. Then, an additional five pulse burst was used for ^{7}Li, ^{57}Fe, ^{59}Co, ^{60}Ni and ^{193}Ir measurements for metal phase identification (the cycling of the magnet to ^{7}Li is for purposes of maintaining mass calibration stability). Thus, the precision of Co, Ni and Ir abundances was sacrificed in favor of better determinations of the interelemental ratios of W–Pt. Counting times were 20 ms/peak with 20–50 scans per point. Analyzing these two mass ranges separately improved precision of the interelement ratios (typically 5%, 1σ). The size of the laser-ablated pit produced was variable, depending on metal grain size, being 25, 50 or 100 μm in diameter and ~25 μm deep. Intensities were blank corrected, and converted to concentrations using sensitivity factors derived from Filomena (North Chile) IIA and Hoba IVB iron meteorites [26,28]. All concentrations were calculated assuming that Fe, Co and Ni total to 100%. Replicate analysis of the Filomena IIA iron using a 25 μm laser spot are given in Table 1. The average of the first five analyses in Table 1 was used to derive sensitivity factors for that dataset. All nine analyses can be used for estimating the precision, but only the last four are useful in estimating accuracy. In Table 1, precision of Co, Ni and Ir abundances (1σ) is 10–20%, while that of the ratios is 5–10%, except where further limited by counting statistics.

3. Results

Data for H chondrite isolated matrix metal are given in Table 2, and data for L and LL chondrite metal are presented together in Table 3. With few exceptions, Os/Ir and Pt/Ir ratios are chondritic. This is consistent with the findings of [19], from

Table 3
Abundances of Co, Ni and Ir, and ratios of W, Re, Os, and Pt to Ir for L and LL chondrite metal determined by LA-ICP-MS

Sample	Co (wt%)	Ni (wt%)	Ir (ppm)	W/Ir	Re/Ir	Os/Ir	Pt/Ir
Mezö-Madaras (L3.7)							
Silicate #14	0.63	7.20	24.5	4.18	0.02	0.35	1.70
Kamacite:							
#4	0.37	5.44	1.4	0.03	0.11	0.96	1.61
#5	*0.80*	*5.03*	*0.5*	*0.09*	*0.60*	*0.17*	*26.7*
#6	0.71	5.37	13.7	0.005	0.11	0.98	1.81
#10	0.88	5.10	3.0	0.033	0.07	1.01	1.10
#11	0.94	4.73	5.1	0.022	0.11	0.97	1.39
#12	0.46	5.77	3.8	0.85	0.28	0.06	3.78
#13	0.41	5.73	2.4	0.96	0.18	0.99	3.37
Taenite:							
#1	0.02	49.9	3.5	0.026	0.10	1.54	3.38
#2	0.75	17.4	4.0	0.005	0.20	1.31	1.45
#3	0.90	13.1	3.0	0.052	0.26	1.09	1.86
#7	0.14	49.5	14.7	0.003	0.09	1.47	1.91
#8	0.68	18.9	10.9	0.005	0.12	1.20	1.68
#9	0.59	8.07	5.5	0.005	0.11	0.96	1.96
Bulk metal [11,13]	0.62	13.2	4.6	0.063	0.10	1.09	2.39
Alfianello (L6)							
Kamacite:							
#2	0.75	4.89	7.28	0.25	0.11	1.30	1.87
#3	0.73	4.89	7.08	0.25	0.13	1.14	1.81
#8	0.78	5.89	5.68	0.30	0.15	1.16	1.63
#10	0.77	5.41	5.36	0.26	0.14	1.23	1.89
#12	0.66	5.01	6.40	0.25	0.12	1.19	1.59
#13	0.66	4.82	3.26	0.51	0.28	0.87	3.20
Taenite:							
#1	0.36	19.9	10.2	0.16	0.10	1.19	1.56
#5	0.43	14.0	7.67	0.23	0.12	1.25	1.32
#6	0.43	26.0	11.1	0.27	0.11	1.18	1.27
#7	0.28	18.6	8.17	0.18	0.09	1.14	1.34
#9	0.29	18.9	4.56	0.39	0.21	1.54	2.11
#11	0.23	26.3	3.35	0.45	0.22	1.22	2.81
#14	0.57	12.7	7.61	0.26	0.15	1.09	2.35
#15	0.24	32.6	4.35	0.40	0.19	1.11	2.07
#16	*0.33*	*27.2*	*0.78*	*3.84*	*1.12*	*0.49*	*15.3*
#17	0.39	16.8	3.75	0.54	0.24	1.16	2.84
Bulk metal [11,13]	0.74	13.0	5.1	0.27	0.13	1.14	2.73
Parnallee (LL3.6)							
Kamacite:							
#3	0.71	7.10	3.33	0.20	0.12	0.80	1.76
#4	0.79	4.28	1.85	0.16	0.16	1.14	2.21
#5	0.78	6.28	4.99	0.05	0.13	1.18	1.45
#6	0.86	6.03	1.41	0.48	0.17	0.85	2.61
#7	0.42	7.68	2.59	0.24	–	3.80	0.98
#8	*0.07*	*3.50*	*0.66*	*0.37*	–	*1.33*	*2.29*
#1 taenite	0.18	29.1	9.28	0.18	0.19	1.36	2.87
#2 plessite?	0.63	12.1	1.68	4.72	0.24	1.58	3.22
Bulk metal [11,13]	0.73	15.8	4.4	0.065	0.11	1.16	2.39

Table 3 *(continued)*
Abundances of Co, Ni and Ir, and ratios of W, Re, Os, and Pt to Ir for L and LL chondrite metal determined by LA-ICP-MS

Sample	Co (wt%)	Ni (wt%)	Ir (ppm)	W/Ir	Re/Ir	Os/Ir	Pt/Ir
Soko-Banja (LL4)							
Kamacite:							
#1	2.29	3.02	3.29	0.23	0.32	0.79	3.43
#2	1.85	3.66	4.08	0.10	0.31	1.31	1.64
#4	1.72	3.75	7.23	0.14	0.10	1.26	0.93
#5	1.61	3.64	6.94	0.08	0.19	1.16	1.73
#7	1.72	7.69	8.66	0.06	0.20	1.01	1.85
#8	1.67	4.47	1.29	0.52	1.70	0.84	13.4
#9	1.88	4.37	2.41	0.14	0.14	1.12	2.74
#10	1.77	3.36	4.42	0.10	0.31	1.18	2.20
#11	0.28	0.62	1.60	0.56	0.07	1.07	0.37
#12	1.89	4.15	16.3	0.02	0.12	0.92	1.44
Bulk metal [12,14]	1.11	26.2	8.2	0.078	0.11	1.06	2.32
Average L3 metal [17]	0.574	15.4	4.20	0.064	0.10	1.088	2.50
Average L4–6 metal [17]	0.633	15.8	4.70	0.265	0.13	1.047	2.23
Bulk L chondrites[a]	0.060	1.23	0.512	0.22	0.082	1.066	2.14
Average LL3 metal [17]	0.837	22.0	6.64	0.048	0.098	1.072	2.61
Average LL4–6 metal [17]	1.07	33.2	8.82	0.19	0.135	1.130	2.48
Bulk LL chondrites[a]	0.049	1.01	0.358	–	0.092	1.081	2.36

[a] Bulk L and LL chondrite abundances from [30], except Os/Ir ratio and Co, Ni and Ir abundances from [61].
Metal grains with extremely low Ir abundances are italicized. Sources of meteorite specimens: Mezö-Madaras (Me 1607), Alfianello (Me 1387), Parnallee (Me 1847), and Soko-Banja (Me 319) from the Field Museum of Natural History, Chicago, IL, USA.

SIMS measurements of the Os, Ir, Pt and Au abundances in ordinary chondrite metal. Metal from UOC exhibits three orders of magnitude variability in W/Ir ratios, and these are shown vs. Re/Ir on a logarithmic scale in Fig. 1. Metal from EOC exhibits a correlation between W/Ir ratios and Re/Ir ratios (Fig. 2). Figs. 3 and 4 show histograms of the distribution of W/Ir and Re/Ir ratios in OC metal, according to petrologic type. Aspects of the data are discussed in further detail below.

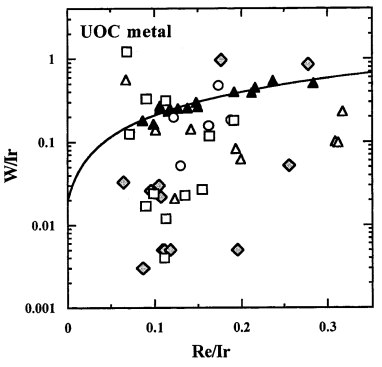

Fig. 1. W/Ir vs. Re/Ir for UOC metal. Metal from Alfianello (L6; kamacite and taenite: solid triangles), with linear regression (bold curve), is shown for comparison. Tieschitz (H3.4): open squares; Mezö-Madaras (L3.7): gray diamonds; Parnallee (LL3.6): open circles; Soko-Banja (LL4): open triangles. Note the large range in W/Ir ratios of UOC metal compared with the narrow range of EOC metal.

3.1. Tieschitz (H3.4)

In kamacite grains from Tieschitz, the W/Ir ratios vary by over two orders of magnitude, and are mostly subchondritic (Fig. 1). One analysis of kamacite (#18) and one of taenite (#23) have Ir contents (0.01 ppm) that are very low for chondritic metals. We propose that metal with such low Ir abundances might have formed by desulfurization of troilite, as troilite has very low PGE contents. The abundances of Co and Ni in Tieschitz metal analyses reported here are similar to the ranges reported previously in the literature [29]. The siderophile element composition of bulk metal separated from Tieschitz [12,14] compares well with individual metal grain analyses

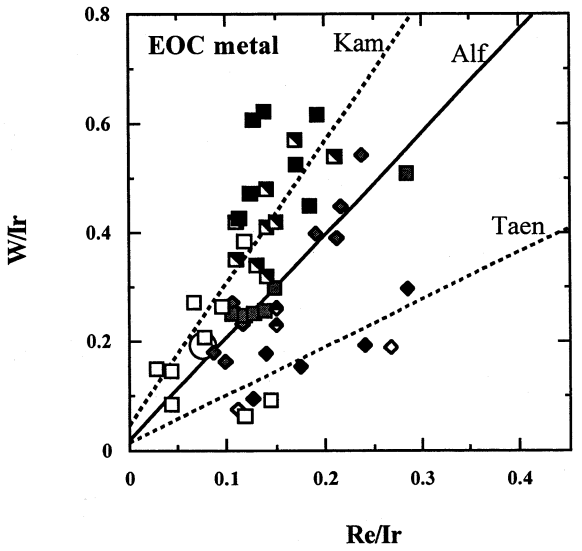

Fig. 2. W/Ir vs. Re/Ir for equilibrated ordinary chondrite (EOC) metal, with kamacite (squares) and taenite (diamonds) shown separately. Weston (H4): open squares/diamonds; Allegan (H5): solid squares/diamonds; Kernouve (H6): half-filled squares/diamonds; Alfianello (L6): gray squares/diamonds; CI chondrite [31]: large open circle. Kam: regression through H chondrite kamacite ($r^2 = 0.5$); Alf: regression through Alfianello kamacite and taenite ($r^2 = 0.9$); Taen: regression through Allegan taenite ($r^2 = 1.0$). The lower regression coefficient for H chondrite kamacite is due to larger scatter in the Weston H4 data. Weston H4 taenite plots along the Allegan taenite line, but Kernouve H6 taenite does not, neither of which were included in the regression.

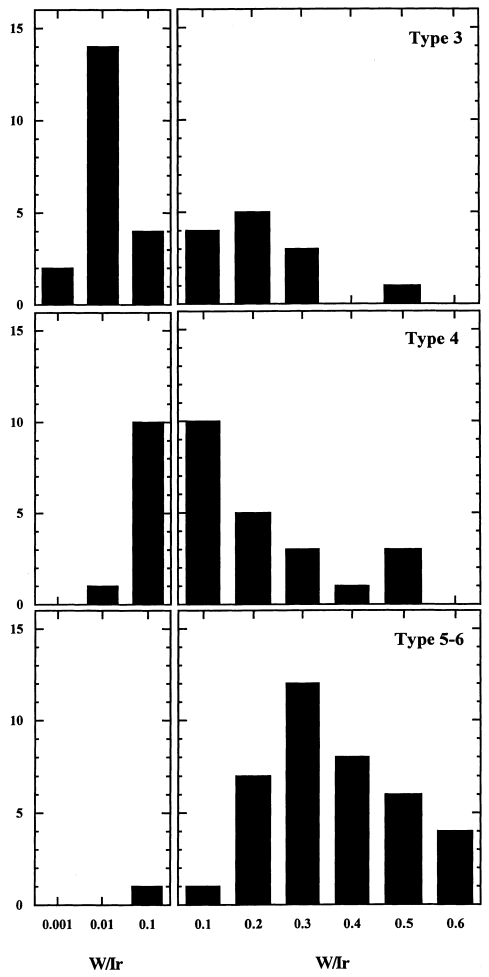

Fig. 3. Histograms showing the distribution of W/Ir ratios in ordinary chondrite metal. Type 3, Type 4 and Type 5–6 are shown in separate panels (W/Ir ratios > 0.6 were omitted). Note that (i) the W/Ir scale is logarithmic in the left panel from 0.001 to 0.1, and linear in the right panel from 0.1 to 0.6; (ii) one component of Type 3 metal has W/Ir < 0.1, another has W/Ir between 0.1 and 0.3, similar to that of Type 4 metal; (iii) Type 5–6 metal is significantly enriched in W relative to chondritic W/Ir = 0.19 [31].

reported in Table 2. The abundance of Ir in Tieschitz metal determined by LA-ICP-MS ranges from 0.5 to 7.0 ppm, a factor of 14, likely reflecting the unequilibrated nature of this chondrite.

3.2. Equilibrated H chondrites

Isolated matrix metal grains ranging in size from 100 to 500 μm were analyzed in Weston (H4) and the results are presented in Table 2. The range of Ir abundances in Weston metal is 2.1–13.0 ppm, a factor of about 6. Taenite #14, the grain with the lowest Ir content, was a small (= 50 μm) grain from a chondrule interior. It exhibits very high W/Ir and Pt/Ir ratios, and even its Os/Ir is almost twice chondritic. Allegan (H5) and Kernouve (H6) exhibit lower ranges in their Ir abundances, with kamacite from Allegan exhibiting uniform Ir and a distinct kamacite–taenite fractionation similar to that observed in iron meteorites. In kamacite from Allegan and Kernouve, there is little variation with W/Ir = 0.53 ± 0.08 (1σ) and 0.43 ± 0.09, respectively, compared with W/Ir = 0.33 in bulk H chondrites [30].

Fig. 2 shows that W/Ir ratios both in kamacite

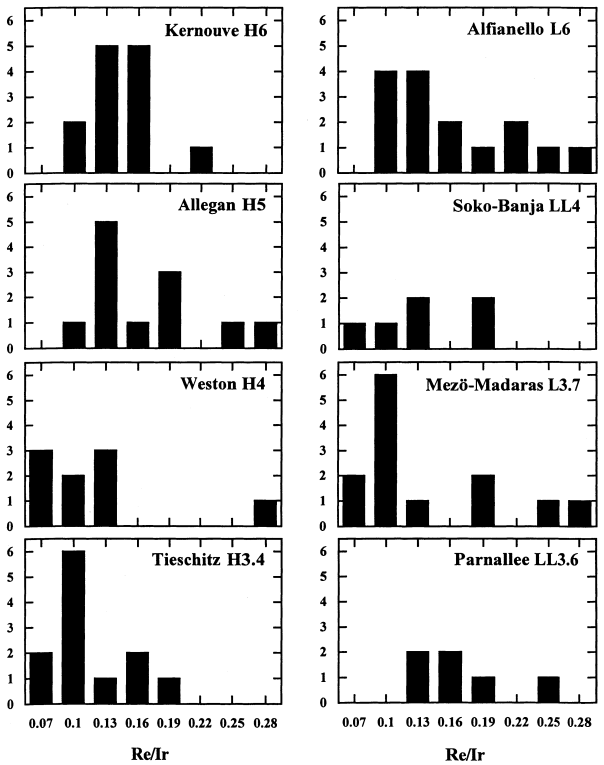

Fig. 4. Histograms showing the distribution of Re/Ir ratios in ordinary chondrite metal for each of the eight chondrites studied, ordered by petrologic type (Re/Ir ratios >0.28 were omitted, and four ratios <0.07 in Weston were also omitted). The CI value is Re/Ir = 0.076 [31], and the mean bulk chondrite metal Re/Ir = 0.10 [11–17]. Note that Re/Ir in Type 5–6 is peaked at 0.13–0.16. There are insufficient data for Parnallee and Soko-Banja to determine the shape of the histogram for these chondrites.

and in taenite from equilibrated H chondrites are correlated with Re/Ir ratios. The line labeled 'Kam' in Fig. 2 is a regression through kamacite compositions of Weston, Allegan and Kernouve, which defines an approximately chondritic W/Re = 2.6. For comparison, CI chondrite W/Re = 2.53 [31]. The line labeled 'Taen' in Fig. 2 is a regression through taenite compositions from Allegan, defining a W/Re = 0.88. In Allegan, kamacite and taenite exhibit similar ranges of Re/Ir, and at the same Re/Ir, W is preferentially concentrated in kamacite by a factor of three relative to taenite, consistent with the bcc structure of metallic W. This feature of W partitioning in Allegan (and partly in Weston) is not well developed in Kernouve metal. Both Allegan and Kernouve metal exhibit systematically higher W/Ir and Re/Ir than bulk metal [12,14], which cannot be accounted for by the presence of taenite, since taenite is a minor fraction (7–14%, estimated by mass balance) of both chondrites. Further, bulk metal W/Ir reported by [17] is similar to that reported by [14] for separated H chondrite metal. The presence of a low W/Ir phase in the bulk metal fraction studied by [14,17] is required [21], but has not been identified here by microanalysis. The W/Ir (0.4–0.5) and Re/Ir (0.15) ratios of average EOC metal determined here (Figs. 3 and 4) are about twice CI values (W/Ir = 0.19, Re/Ir = 0.076) [31], largely due to a deficiency of Ir in the isolated matrix metal. The Ir-rich complementary material (probably low W/Ir) was apparently partially sampled by the separated bulk metal fractions of [12–15,17].

3.3. Unequilibrated L and LL chondrites

Fig. 1 shows that the unequilibrated L and LL

chondrites, Mezö-Madaras (L3.7) and Parnallee (LL3.6), exhibit a broad range of W/Ir ratios, similar to that of Tieschitz (H3.4). A single grain (#5) of metal in Mezö-Madaras exhibits <1 ppm Ir, with high Re/Ir and Pt/Ir, and low Os/Ir (Table 3). A silicate-rich portion of a chondrule was analyzed (#14) where the observable metal fraction was low. The abundances were calculated as Fe+Co+Ni = 100%, but the ratios to Ir are not affected by this normalization. The Ni content indicates that the analysis is dominated by metal grains, but the W/Ir ratio is high indicating that lithophile W is being measured. The bulk composition of separated metal reported for Mezö-Madaras [11,13] is in reasonable agreement with the individual grain measurements in Table 3. However, for Parnallee, metal with higher W/Ir and Re/Ir ratios than the bulk metal was oversampled here. The range of kamacite Ir abundances is 1.4–13.7 ppm in Mezö-Madaras metal, a factor of about 10, similar to that observed in Tieschitz (H3.4).

3.4. Equilibrated L and LL chondrites

Fig. 1 shows that Soko-Banja (LL4) exhibits a behavior intermediate between the UOC and Alfianello (L6), which exhibits a tight W/Ir vs. Re/Ir correlation. Fig. 2 shows that the kamacite–taenite partitioning exhibited by Allegan (H5) is not evident in Alfianello (L6), where both kamacite and taenite define the same trend labeled 'Alf' in Fig. 2. Alfianello kamacite compositions cluster tightly around separated bulk metal [11,13]. The range of Ir abundances in kamacite from Alfianello is quite limited, 3.3–7.3 ppm, with higher ranges in taenite, 3.4–11.1 ppm, compatible with metamorphic equilibration of kamacite Ir abundances. Metamorphism narrows the range of Ir variations in EOC relative to UOC, but substantial variation persists even in the most highly equilibrated chondrites. A single grain (#11) in Soko-Banja (LL4) exhibits low Ni, Re and Pt, and is complementary to grains with high Re/Ir and Pt/Ir ratios. Like the equilibrated H chondrites, Alfianello exhibits W/Ir and Re/Ir ratios that are about twice chondritic (Figs. 3 and 4), while its W/Re = 2.1.

4. Discussion

4.1. Tungsten cosmochemistry

Tungsten is a refractory metal with a condensation temperature from a gas of solar composition comparable to that of Re and Os, and higher than that of Ir [32,33]. Tungsten is more easily oxidized than Re, or the platinum group elements, and its metal–metal oxide transformation occurs under redox conditions between the Fe–FeO and Co–CoO buffers [34]. In gases that are more oxidizing than solar composition, W will form gaseous oxides (WO_2, WO_3) that are volatile, and W depletions have been described from metal in some calcium–aluminum inclusions (CAIs) [33,35]. Parent body processes can also oxidize W, which then behaves as an incompatible lithophile element. Thus, W partitions between metal and silicate in planetary processes, and the metal–silicate partition coefficient, $D_{m/s}$, has been determined as a function of temperature and oxygen fugacity at ambient pressure [36]. One important source of chondrite metal is the process of chondrule formation, where initially oxidized (FeO-rich) material is reduced during melting [46,63]. The composition of metal in equilibrium with a molten chondrule was calculated as a function of pO_2 using data from [36], and is shown in Fig. 5. The calculation was performed at 1573 K and 1873 K, the experimental run temperatures of Schmidt et al. [36], who noted that W changes its behavior at higher temperatures, perhaps due to a change in coordination number. Similarly, W is reduced during subsolidus processes of chondrite metamorphism at $T \sim 700$–1200 K that produced metallic Fe by reduction of FeO-bearing silicates, but the exact relation between W in metal and pO_2 under metamorphic conditions is not experimentally calibrated at present.

4.2. Tungsten microdistribution in ordinary chondrite metal

In this section, the modification of W/Ir and Re/Ir ratios in OC metal established during chondrule formation (Fig. 5) by metamorphic equilibration is discussed. Figs. 1 and 2 show W/Ir vs.

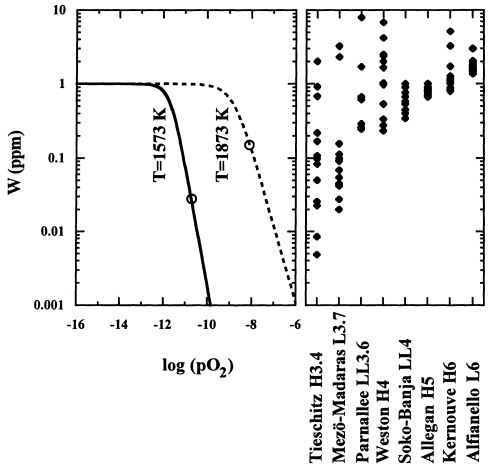

Fig. 5. (a) Calculated W abundance in a metal grain in equilibrium with silicate as a function of pO_2 at $T = 1573$ K and $T = 1873$ K, using W metal–silicate partition coefficients from [36]. The maximum abundance of W in Fe metal based on bulk H chondrite W = 160 ppb [30], and a metal content of 16 wt% [62] is 1 ppm. The circles indicate canonical solar nebula pO_2 at those temperatures [64]. (b) W abundances in kamacite grains calculated from W/Ir ratios and Ir abundances in Tables 2 and 3. Metal grains that plot above 1 ppm probably formed by reduction of silicate after first-stage metal extraction. H5–6 chondrite metal plots close to the 1 ppm W abundance, while Alfianello L6 has higher W abundances reflecting the general Fe depletion of L chondrite metal relative to Ni and other siderophiles.

Re/Ir variations in H and L/LL chondrite metal. Literature values of bulk analyses of separated metal [11–14,17] are presented in Tables 2 and 3. The UOC metal from all chemical classes exhibits a large range in W/Ir ratios, including some analyses that are below the detection limit, 0.003, for the analytical procedure used here. Bulk metal W/Ir of Tieschitz, Mezö-Madaras and Parnallee are significantly lower than those reported for Allegan, Kernouve and Alfianello [11–14], indicating that metamorphism resulted in a net transfer of W from oxidized phases to OC metal, in addition to reducing the spread in W/Ir ratios. Fig. 3 shows that this is also observed in an histogram of W/Ir where Type 3, Type 4 and Type 5–6 metal are depicted separately.

Fig. 4 shows a histogram for Re/Ir for each chondrite, and demonstrates that Re/Ir does not increase with metamorphic grade to the same extent as W/Ir. The mean Re/Ir ratio of Type 3 chondrite metal is about 0.10 (similar to bulk H chondrites [30]), which increases to 0.14 ± 0.02 in Type 5–6 metal, in both kamacite and taenite. Metal from the Type 4 chondrites, Weston and Soko-Banja, appears to be intermediate in W/Ir and Re/Ir ratios (Figs. 3 and 4). Thus, the transfer of W from silicates to matrix metal takes place mostly in Type 3.0–4 chondrites, with no observable change in Type 5–6 chondrites.

In EOC metal, there is a correlation between W/Ir and Re/Ir ratios (Fig. 2) indicating that the observed variations, including the Re/Ir enrichment observed in EOC metal [12,17–18], are the result of reduction of W and Re from silicate phases during metamorphic equilibration. Since W is more lithophile than Re, the effect is more pronounced for W than for Re. The relative order of the metal–metal oxide pairs in terms of chemical potentials are $W < Re < Os < Ir < Pt < Au$ [37,38], thus W is the easiest to oxidize. The Re–ReO_2 buffer has $\mu O_2 \approx 45$ kJ/mol higher than that of Ni–NiO [34,37], while W–WO_2 has $\mu O_2 \approx 5$–45 kJ/mol greater than that of Fe–FeO buffer over 700 K $< T <$ 1700 K, and below that of the Co–CoO buffer [34], making W only slightly more siderophile than Fe, and less siderophile than both Co and Ni.

Further, in EOC metal, W/Re ratios are approximately chondritic, while Ir and Os abundances are variably depleted. It is conceivable that Ir and Os were present in both Fe–Ni alloy and as refractory metal nuggets in UOC, as first proposed by [39]. During metamorphism, reduction of FeO from the silicates contributed further Fe to pre-existing metal grains, resulting in dilution of Ir and Os abundances. The presence of W and Re in chondritic relative proportions is possibly related to their original presence in an oxidized form (perhaps in silicates), which either directly contributed to their abundances during reduction, or facilitated the diffusive transport of these elements to the sites of incorporation into metal. The average Ir–Os abundance in OC metal ranges from chondritic to about a factor of two lower than chondritic [21–23]. The superchondritic Re/Os ratios observed by [18] in their ^{187}Re–^{187}Os isotopic studies of separated OC metal were

caused by reduction of Re from the silicate to the metal.

4.3. The nature of the reductant

Reduction during OC metamorphism plays an essential role in establishing the W/Ir and Re/Ir ratios of EOC metal, and the nature of the reductant is considered here. The possible reductants in ordinary chondrites include carbonaceous material (carbides, elemental carbon or organic molecules), phosphides or metal with dissolved Si, P and Cr [46]. Ordinary chondrites contain a few thousand ppm reduced C, including both terrestrial contaminants and indigenous phases [40,41]. Bulk carbon contents of ordinary chondrites are affected by terrestrial contamination and the isotopic composition of indigenous C in OC ($\delta^{13}C \approx -16$ to -27‰ [41]) is very similar to that of C3 pathway organic matter, probably the most ubiquitous source of reduced carbon contamination. Thus, isotopic fingerprinting of the indigenous C is not possible. Stepped combustion techniques [41] yield carbon abundances that do not show systematic trends with metamorphic grade or petrologic type. For example, with the exception of Sharps (C = 27 700 ppm), Grady et al. [41] obtained C ≈ 2200–3700 ppm for H3 chondrites, and C ≈ 1000–3200 ppm for H4–6 chondrites. Results for LL chondrites were more systematic with C ≈ 3000–5400 ppm for LL3.0–3.4, and C ≈ 310–990 ppm for LL4–6. However, the carbon contents of Type 3.0 to Type 3.9 OC falls determined by [40] show no systematic pattern with petrologic type. These results constitute suggestive, but not compelling, evidence for C consumption during metamorphic equilibration in ordinary chondrites.

Certain tracers such as presolar grains and interstellar organic molecules, the carriers of distinct isotopic signatures [42,43], provide better proxy measures of the reductant consumption. *D*/*H* ratios (a proxy for interstellar molecules) of water extracted from UOCs were observed to decrease with increasing metamorphic grade [44]. Huss [25] observed that the abundances of presolar diamond and SiC grains decreased during the initial stages of OC metamorphism in UOC, generally vanishing at about metamorphic grades 3.6–3.8. This was attributed to oxidation of these reduced phases during incipient metamorphism by reaction with FeO in silicates [25]. A more comprehensive study of the abundances of presolar diamond, SiC and graphite abundances in the matrices of UOC showed that abundances of each of the presolar grain types decreased sharply at Type 3.6–3.8, with graphite disappearing by Type 3.1 [42]. Abundance of presolar diamond was initially about 125–177 ppm (about 3–5% of the bulk C) in the least equilibrated UOCs, Semarkona, Krymka and Bishunpur, decreasing by a factor of 10^3 in Type 3.8 UOCs [42]. This process added Fe to OC metal, and based on our data also added W and Re. Likewise, [17] noted that W and Ga were added to bulk OC metal during metamorphism. It is essential to terminate this reduction process, or W would equilibrate throughout the metamorphic episode, contrary to the findings of [4,45]. Given the evidence for consumption of C-bearing phases (presolar grains, interstellar organic molecules) in the earliest stages of metamorphism (Type 3.0–3.8), it is proposed here that exhaustion of the available reductant terminates the process, setting the ^{182}Hf–^{182}W chronometer. This process occurs largely by Type 4 as indicated in Figs. 3 and 4. Analyses of W in bulk metal separates [17] also shows that Type 3 metal is a factor of four lower in W than bulk metal from Type 4–6 chondrites (Tables 2 and 3).

4.4. An interval of metamorphism

The process of metamorphic equilibration, which results in the reduction of FeO-bearing silicates to form metallic Fe, also results in oxidation of highly reduced Cr-, P- and Si-bearing metal grains described by Zanda et al. [46] from UOCs. The P oxidized from OC metal forms phosphate minerals, mainly apatite and merrillite. Goreva and Burnett [47] found that U and Th in OCs, which initially reside in chondrule glass, were transferred to phosphates during metamorphism. Likewise, oxidized W is an incompatible lithophile, and was presumably present in chondrule glasses. Thus, the U–Pb chronometer is initially set during the same process of metamorphic

equilibration that sets the ^{182}Hf–^{182}W chronometer. The Pb closure temperature of apatite was estimated to be 690–750 K, while the peak temperatures attained during metamorphism for Type 5–6 chondrites were estimated to be 950–1200 K [7]. The closure temperature of kamacite or taenite with respect to the diffusivity of W is not known. Experimental determination of the diffusivity of W in Fe–Ni metal at subsolidus temperatures is essential for a more complete interpretation of ^{182}Hf–^{182}W chronology in metamorphosed chondrites.

A $\Delta T = 60$ Myr of H-chondrite metamorphism on a parent-body scale was established from ^{207}Pb–^{206}Pb systematics of EOC phosphates [7] as the time difference between isotopic closure in Type 4 and Type 5–6 chondrites. This range of metamorphic ^{207}Pb–^{206}Pb ages is concordant with ^{129}I–^{129}Xe ages on phosphates and feldspars from the same chondrites [5]. This estimate of timing is in conflict with recent data based on the short-lived ^{182}Hf–^{182}W chronometer that indicated that metal separated from ordinary chondrites of all metamorphic grades exhibited about the same $\varepsilon^{182}W$ [4,45], distinct from OC silicate phases which have radiogenic $\varepsilon^{182}W$ and plot on an isochron defined by whole rock, separated metal and non-magnetic (i.e., silicate) phases [45]. Further, the $\varepsilon^{182}W$ of OC metal is similar to that of iron meteorites indicating that it was isolated from equilibrium with lithophile Hf early in solar system history: ^{182}Hf–^{182}W ages for OC metal from eight Type 4–6 chondrites determined against the least radiogenic W from the IAB iron Arispè are 3–10 Myr, with metal from five chondrites of all petrologic types in the narrower range of 3–5 Myr [4]. This is initially surprising given the degree of W equilibration required to progress from Type 3 chondrites with their large range of W/Ir ratios to Type 4–6 chondrites, with their narrower ranges of W/Ir. We propose that these seemingly contradictory findings can be reconciled if: (1) the onset of metamorphism in the OC parent body occurred at a very early time in solar system history, shortly after accretion, and (2) reduction took place during the initial stages of metamorphism (mainly prior to grade 4), and that most of the reductant was consumed in this phase, so that further exchange of unradiogenic W from metal with radiogenic W in silicate was inhibited. By contrast, the U–Pb chronometer was set during cooling from peak metamorphic temperatures, as phosphates reached their U–Pb closure temperatures [7]. Since there is no change in coordination number of U, Pb, I or Xe, during chondrite metamorphism, these systems respond exclusively to temperature. Thus, the ^{182}Hf–^{182}W chronometer and the U–Pb chronometer date fundamentally different processes, the former marking the onset of metamorphism and the latter marking its termination. The duration of metamorphism is obtained from the time difference between isotopic

Table 4
Intervals of metamorphism (ΔT_m) calculated for individual chondrites as the time difference between ^{207}Pb–^{206}Pb ages [7] and ^{182}Hf–^{182}W ages [4]

Chondrite	^{207}Pb–^{206}Pb age (Myr)	^{182}Hf–^{182}W age (Myr)	ΔT_m (Myr)
Ste. Marguerite (H4)	3.3 ± 0.6	4 ± 2	−1 ± 2
Forest Vale (H4)	5.1 ± 0.7	3 ± 2	2 ± 2
Richardton (H5)	14.6 ± 0.6	3 ± 1	12 ± 1
Nadiabondi (H5)	10.4 ± 3.4	8+4/−3	2 ± 5
Allegan (H5)	15.8 ± 0.7	8+4/−3	8 ± 4
Kernouve (H6)	42.1 ± 0.5	–	–
Barwell (L5–6)	27.8 ± 0.7	2 ± 2	26 ± 2
Tuxtuac (LL5)	22.4 ± 2.1	10 ± 2	12 ± 3
St. Séverin (LL6)	12.4 ± 0.7	5 ± 2	7 ± 2

^{207}Pb–^{206}Pb ages are presented as the time difference between Allende CAIs (4566 Myr) and OC phosphates using the Pb isotopic composition of Canyon Diablo troilite as initial Pb [7].

closure of the ^{207}Pb–^{206}Pb or ^{129}I–^{129}Xe chronometer and the ^{182}Hf–^{182}W chronometer.

Table 4 summarizes the available chondrite data, with metamorphic intervals calculated for each individual chondrite. As an example of the distinction between parent-body metamorphic duration, estimated from the difference in timing of isotopic closure between Type 4 and Type 5–6 chondrites [7], and the metamorphic intervals defined here for individual chondrites (Table 4), consider the three H5 chondrites Nadiabondi, Richardton and Allegan. These exhibit a range of ^{207}Pb–^{206}Pb ages of 10–16 Myr after formation of Allende CAI [7] which, when taken together with the 3–5 Myr ^{207}Pb–^{206}Pb ages of H4 chondrites and the >40 Myr ^{207}Pb–^{206}Pb ages of Type 6 chondrites, appear to be part of a layered parent body with a regular increase in duration of metamorphism with petrologic type. However, the initiation of metamorphism indicated by W isotopic closure is variable giving estimates of the individual ΔT_m of 2–12 Myr (Table 4). This indicates that either: (1) thermal metamorphism did not initiate at the same time everywhere on the H chondrite parent body, or (2) exhaustion of reductants occurred at different rates in individual chondrites.

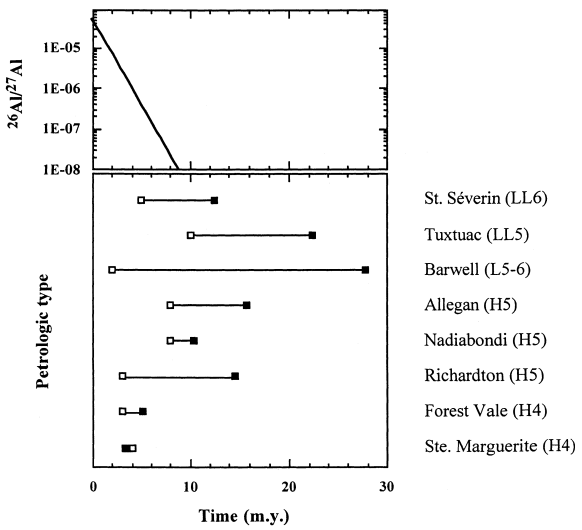

Fig. 6. Schematic illustration of the interval of metamorphism for eight chondrites from Table 4. The upper panel shows ^{26}Al abundance on the same time scale along the abscissa. Five chondrites appear to have been first metamorphosed in a narrow time period, 2–4 Myr, while metal and silicate in Allegan, Nadiabondi and Tuxtuac equilibrated W isotopes until 8–10 Myr. See text for further discussion.

Fig. 6 summarizes the ^{182}Hf–^{182}W ages of EOC metal and the ^{207}Pb–^{206}Pb ages of EOC phosphates. The ^{182}Hf–^{182}W ages of metal from Forest Vale (H4), Ste. Marguerite (H4), Richardton (H5), Barwell (L5–6), and St. Sèverin (LL6) define a narrow band of 3–5 Myr after the differentiation of Arispè (IAB) [4]. It should be noted that an absolute chronology of the ^{182}Hf–^{182}W system has not yet been achieved. No measurements of $\varepsilon^{182}W$ are available for refractory metal from CAIs in Allende or other carbonaceous chondrites, which presents a source of systematic error when comparing ^{182}Hf–^{182}W ages with those based on other short-lived chronometers, e.g., ^{26}Al–^{26}Mg. We will assume for the purposes of Fig. 6 that the time difference between formation of Arispè and that of CAIs is negligible, and it can be constrained as ≤ 3 Myr based on the ^{182}Hf–^{182}W and ^{207}Pb–^{206}Pb ages of Ste. Marguerite. Also depicted in Fig. 6 is the abundance of ^{26}Al as a function of time since the formation of Allende CAIs [52,65]. The early group of ^{182}Hf–^{182}W ages (Ste. Marguerite, Forest Vale, Richardton, Barwell and St. Sèverin) is compatible with metamorphism on parent bodies heated by ^{26}Al, but the late metamorphism observed in Allegan, Nadiabondi and Tuxtuac requires the operation of additional processes, possibly including impact heating. Further evidence for distinct expressions of metamorphism is provided by the well developed kamacite–taenite W partitioning in Allegan (H5) metal relative to that from Kernouve (H6) and Alfianello (L6).

As indicated by recent models [48], the timescale of the accretion disk phase of the solar system is short (<1 Myr) compared with metamorphic timescales of chondrite parent bodies. Further, to avoid partial melting of the ordinary chondrite parent bodies by heat generated from the decay of ^{26}Al ($t_{1/2} = 0.7$ Myr), these would have formed >2 Myr after Allende CAIs, as argued by Woolum and Cassen [49]. The timescale over which ^{26}Al releases its thermal energy is ~ 5–6 Myr (Fig. 6). Thus, using the five chondrites

with early ^{182}Hf–^{182}W ages, the inferred timescales of metamorphism for the ordinary chondrite parent bodies are consistent with thermal energy derived from ^{26}Al decay, a conclusion supported by ^{26}Al–^{26}Mg systematics of Al-rich chondrules from OCs [50,65]. Cooling through the Pb closure temperature of phosphates for the Type 4 chondrites, Forest Vale and Ste. Marguerite, indicates that this had occurred by $\Delta T = 5$ Myr. This is consistent with the presence of ^{26}Mg excesses correlated the Al/Mg ratios in feldspar grains from Ste. Marguerite and Forest Vale, which yield $\Delta T \sim 6$ Myr for cooling through the Mg closure temperature of feldspar [51,52]. Based on ^{26}Al–^{26}Mg systematics of a larger set of OC chondrites, Huss et al. [65] similarly concluded that metamorphism of Type 4 OCs was completed by 5–6 Myr after CAI formation.

The existence of a chemical reaction (i.e., C reduction of WO_2/WO_3) that is initiated by metamorphic heating, but turned off by the exhaustion of one of the reactants (C) before reaching peak temperature, is of fundamental significance to cosmochronology. That such a reaction can set a chronometer, in this case the ^{182}Hf–^{182}W chronometer, is identified here for the first time to our knowledge. All known metamorphic geochronometers are based on the closure temperature concept [8,9] that record the time since cooling through a closure temperature from peak temperatures. Thus, this is also the first instance known where a chronometer is set by the onset of metamorphism, and can thus yield a more direct measure of the duration of metamorphism when combined with one of several available metamorphic geochronometers based on closure temperature, including ^{40}Ar–^{39}Ar, ^{87}Rb–^{87}Sr or $^{238,235}U$–$^{207,206}Pb$. It is important to observe here that the ^{187}Re–^{187}Os chronometer in ordinary chondrites is also set by the reduction process, and that ^{187}Re–^{187}Os ages of ordinary chondrites [18] must reflect the initiation of metamorphism, as well. Thus, the short-lived ^{182}Hf–^{182}W and the long-lived ^{187}Re–^{187}Os are contemporaneous.

The application of the ^{182}Hf–^{182}W chronometer is presently limited to cosmochronology, and it is probably further limited by instances where available reductant is almost completely consumed early in the metamorphic process. Otherwise, W would probably continue to be reduced from the silicate phases where ^{182}W was being produced by radioactive decay of its parent ^{182}Hf, and added to the metal phase. Thus, we would predict W isotopic equilibration of metal and silicate from metamorphosed carbonaceous chondrites or ureilites and other materials in which reductant remained in excess of that which is consumed by FeO reduction. A potential analog of this system may be found in the ^{187}Re–^{187}Os chronology of reduced terrestrial sediments, where ^{187}Re–^{187}Os ages may reflect the onset of metamorphism rather than its termination. Existing ^{187}Re–^{187}Os studies of terrestrial sediments have been restricted to determining the timing of deposition of black shales [53,54], rather than the ages of metamorphism. Black shales are very C-rich, but metasediments of lower C content are far more common and their ^{187}Re–^{187}Os systematics potentially could be used to determine the timing of initiation of metamorphism in major mountain belts. This remains to be explored further.

4.5. Ordinary chondrite metal composition as a proxy for Re/Os of the Earth's core

Recent work on the ^{187}Re–^{187}Os systematics of terrestrial basalts has revealed the presence of excess radiogenic $^{187}Os/^{188}Os$ in ocean island basalts [55,56]. One set of models for this observation postulates that Os from the terrestrial outer core is physically entrained in [55,57], or isotopically exchanged [58] with, the mantle sources of OIB at the core–mantle boundary. Models for the isotopic evolution of $^{187}Os/^{188}Os$ in the Earth's core have used the Re/Os of H5 chondrite metal as representative of bulk core [55–57], rather than CI chondrite values (Re/Os = 0.075 [31]), on the argument that the Earth accreted from volatile depleted material like H-chondrites [55,56]. Since the Re/Os ratio used in these models (0.083–0.088 [55–57]) is a factor of 1.1–1.2 × CI the amount of fractional crystallization required to achieve a model outer core Re/Os ratio is lower for given values of the solid metal–liquid metal partition coefficients for Re and Os. Fig. 4 shows that individual metal grains in Allegan H5 and Ker-

nouve H6 exhibit a range of Re/Ir ratios, mostly 1.7×CI or higher. From data in Table 2, mean Re/Os ratios of 0.147 and 0.133 were calculated for metal from Allegan H5 and Kernouve H6, respectively. These high Re/Os ratios are a specific feature of EOC metal due to metamorphic processes, calling into question the choice of H5 chondrite metal composition as a proxy for that of the Earth's bulk core. The use of CI values for bulk core (e.g., [58]) is recommended.

5. Conclusions

The processes that formed ordinary chondrite matrix metal occurred under conditions where W was initially lithophile, and produced a large range in the initial W/Ir ratios of chondrite metal, with initial Re/Ir ratios of ~0.10. Metamorphic equilibration reduced the grain to grain variability of the metal, and added Fe, W and Re from nonmetallic phases. Thus, the W/Ir and Re/Ir ratios of EOC metal are about twice that of CI chondrites. This is due in large part to a factor of two deficiency of Ir in the metal, which is present elsewhere in the chondrites. The metamorphic equilibration, occurring mainly in petrologic Type 3–4, involved reduction of oxidized Fe, W, and Re by carbonaceous material in the matrix, the process being terminated by consumption of the available reductant. For a Type 5–6 chondrite, this would occur while the chondritic material was heated past Type 4 conditions. There is no dependence on chemical class, with these results being similar for H, L and LL chondrites. The implications of this process for the ^{182}Hf–^{182}W and ^{187}Re–^{187}Os chronometers are that the chronometers were set during the initial stages of metamorphic equilibration (Type 3.0–4) rather than during cooling from peak temperatures, and hence give ages that are earlier than those obtained from isotopic closure of ^{207}Pb–^{206}Pb or ^{129}I–^{129}Xe systems in chondritic phosphates, thus resolving the discrepancy between these chronometers. The recognition of isotopic closure during reduction for the two siderophile element chronometers allows the determination of an interval of metamorphism derived from the time difference between the ^{182}Hf–^{182}W age and the ^{207}Pb–^{206}Pb (or ^{129}I–^{129}Xe) age. The understanding of the behavior of Re and W in metal during OC metamorphism presented here reconciles the apparent contradiction between ages derived from different chronometers, and couples a short-lived with a long-lived chronometer from which absolute ages can ultimately be derived. Further, ^{182}Hf–^{182}W ages of some ordinary chondrite metal indicate the initiation of OC metamorphism at 3–5 Myr during which ^{26}Al was a viable heat source.

The use of Re/Os ratios of H5 metal as a proxy for that of the Earth's core is shown here to be incorrect, since ordinary chondrite metal has Re/Os ratios significantly different from that of bulk chondrites. This does not invalidate the core–mantle interaction hypothesis, but requires an upwards revision of the solid metal-liquid metal partition coefficients used to derive the inferred radiogenic Os isotopic composition of the outer core.

Acknowledgements

This study was supported by NASA NAG5-9800 to M.H. The following meteorite specimens were generously provided by Meenakshi Wadhwa (Field Museum of Natural History, Chicago, IL, USA): Alfianello, Allegan, Mezö-Madaras, Parnallee, Soko-Banja, and Weston. Tieschitz (L3443) was graciously provided by Gero Kurat, Naturhistorisches Museum, Vienna, Austria. Tracy Rushmer kindly provided fragments of Kernouve (H6) USNM 359 starting material from her experiments, the original source of which is the Smithsonian Institution, Washington, DC, USA. Filomena (North Chile, USNM 1334) was provided by the Smithsonian Institution's National Museum of Natural History, courtesy of Linda Schramm and Glenn MacPherson. R.N. Clayton is thanked for comments on the manuscript which significantly improved its quality. The manuscript benefited from reviews by Alan D. Brandon, Der-Chuen Lee and Sara S. Russell. *[BW]*

References

[1] G.J. Wasserburg, D.A. Papanastassiou, Some short-lived nuclides in the early solar system – a connection with the placental ISM, in: C.A. Barnes, D.D. Clayton, D.N. Schramm (Eds.), Essays in Nuclear Astrophysics, Cambridge University Press, Cambridge, 1982, pp. 77–140.

[2] F.A. Podosek, E.K. Zinner, G.J. MacPherson, L.L. Lundberg, J.C. Brannon, A.J. Fahey, Correlated study of initial $^{87}Sr/^{86}Sr$ and Al-Mg systematics and petrologic properties in a suite of refractory inclusions from the Allende meteorite, Geochim. Cosmochim. Acta 55 (1991) 1083–1110.

[3] G.W. Lugmair, A. Shukolyukov, Early solar system events and timescales, Meteorit. Planet. Sci. 36 (2001) 1017–1026.

[4] D.-C. Lee, A.N. Halliday, Hf-W isotopic evidence for rapid accretion and differentiation in the early solar system, Science 274 (1996) 1876–1879.

[5] R.H. Brazzle, O.V. Pravdivtseva, A.P. Meshik, C.M. Hohenberg, Verification and interpretation of the I-Xe chronometer, Geochim. Cosmochim. Acta 63 (1999) 739–760.

[6] T. LaTourrette, G.J. Wasserburg, Mg diffusion in anorthite: implications for the formation of early solar system planetesimals, Earth Planet. Sci. Lett. 158 (1998) 91–108.

[7] C. Göpel, G. Manhès, C.J. Allègre, U-Pb systematics of phosphates from equilibrated ordinary chondrites, Earth Planet. Sci. Lett. 121 (1994) 153–171.

[8] M.H. Dodson, Closure temperature in cooling geochronological and petrological systems, Contrib. Mineral. Petrol. 40 (1973) 259–274.

[9] I. McDougall, M.T. Harrison, Geochronology and Thermochronology by the $^{40}Ar/^{39}Ar$ Method, 2nd edn., Oxford University Press, Oxford, 1998, 269 pp.

[10] G.J. Wasserburg, D.A. Papanastassiou, H.G. Sanz, Initial strontium for a chondrite and the determination of a metamorphism or formation interval, Earth Planet. Sci. Lett. 7 (1969) 33–43.

[11] E. Rambaldi, Trace element content of metals from L-group chondrites, Earth Planet. Sci. Lett. 31 (1976) 224–238.

[12] E.R. Rambaldi, Trace element content of metals from H- and LL-group chondrites, Earth Planet. Sci. Lett. 36 (1977) 347–358.

[13] E.R. Rambaldi, The content of Sb, Ge and refractory siderophile elements in metals of L-group chondrites, Earth Planet. Sci. Lett. 33 (1977) 407–419.

[14] E.R. Rambaldi, M. Cendales, Tungsten in ordinary chondrites, Earth Planet. Sci. Lett. 36 (1977) 372–380.

[15] E.R. Rambaldi, M. Cendales, R. Thacker, Trace element distribution between magnetic and non-magnetic portions of ordinary chondrites, Earth Planet. Sci. Lett. 40 (1978) 175–186.

[16] P. Kong, M. Ebihara, Metal phases of L chondrites: their formation and evolution in the nebula and in the parent body, Geochim. Cosmochim. Acta 60 (1996) 2667–2680.

[17] P. Kong, M. Ebihara, The origin and nebular history of the metal phase of ordinary chondrites, Geochim. Cosmochim. Acta 61 (1997) 2317–2329.

[18] J.H. Chen, D.A. Papanastassiou, G.J. Wasserburg, Re-Os systematics in chondrites and the fractionation of the platinum group elements in the early solar system, Geochim. Cosmochim. Acta 62 (1998) 3379–3392.

[19] W. Hsu, G.R. Huss, G.J. Wasserburg, Ion probe analyses of PGEs in metallic phases of chondrites: implications for the origin of chondritic metals, Lunar Planet. Sci. Conf. XXIX, 1998, CD-ROM abstracts, LPI, Houston, TX, #1939.

[20] W. Hsu, G.R. Huss, G.J. Wasserburg, Ion probe measurements of Os, Ir, Pt, and Au in individual phases of iron meteorites, Geochim. Cosmochim. Acta 64 (2000) 1133–1147.

[21] M. Humayun, A.J. Campbell, Re, Os, and Ir fractionation in ordinary chondrite metal, Lunar Planet. Sci. Conf. XXXI, 2000, CD-ROM abstracts, LPI, Houston, TX, #2032.

[22] M. Humayun, A.J. Campbell, Tungsten microdistribution in ordinary chondrite metal, Meteorit. Planet. Sci. 35 (2000) A79.

[23] M. Humayun, A.J. Campbell, The duration of ordinary chondrite metamorphism inferred from tungsten microdistribution in OC metal, Lunar Planet. Sci. Conf. XXXII, 2001, CD-ROM abstracts, LPI, Houston, TX, #2102.

[24] D.W. Sears, J.N. Grossman, C.L. Melcher, L.M. Ross, A.A. Mills, Measuring metamorphic history of unequilibrated ordinary chondrites, Nature 287 (1980) 791–795.

[25] G.R. Huss, Ubiquitous interstellar diamond and SiC in primitive chondrites: abundances reflect metamorphism, Nature 347 (1990) 159–162.

[26] A.J. Campbell, M. Humayun, Trace element microanalysis in iron meteorites by laser ablation ICP-MS, Anal. Chem. 71 (1999) 939–946.

[27] A.J. Campbell, M. Humayun, A. Meibom, A.N. Krot, K. Keil, Origin of zoned metal grains in the QUE94411 chondrite, Geochim. Cosmochim. Acta 65 (2001) 163–180.

[28] A.J. Campbell, M. Humayun, M.K. Weisberg, Siderophile element constraints on the formation of metal in the metal-rich chondrites Bencubbin, Weatherford, and Gujba, Geochim. Cosmochim. Acta 66 (2002) 647–660.

[29] R. Hutchison, A.W.R. Bevan, S.O. Agrell, J.R. Ashworth, Thermal history of the H-group of chondritic meteorites, Nature 287 (1980) 787–790.

[30] J.T. Wasson, G.W. Kallemeyn, Compositions of chondrites, Phil. Trans. R. Soc. London A325 (1988) 535–544.

[31] E. Anders, N. Grevesse, Abundances of the elements: Meteoritic and solar, Geochim. Cosmochim. Acta 53 (1989) 197–214.

[32] P.J. Sylvester, S.B. Simon, L. Grossman, Refractory inclusions from the Leoville, Efremovka, and Vigarano C3V chondrites: Major element differences between Types A and B, and extraordinary refractory siderophile element composition, Geochim. Cosmochim. Acta 57 (1993) 3763–3784.

[33] A.J. Campbell, S.B. Simon, M. Humayun, L. Grossman, Chemical evolution of metal in refractory inclusions in CV3 chondrites, Geochim. Cosmochim. Acta 66 (2002) in press.
[34] H.St.C. O'Neill, M.I. Pownceby, Thermodynamic data from redox reactions at high temperatures. I. An experimental and theoretical assessment of the electrochemical method using stabilized zirconia electrolytes, with revised values for the Fe-'FeO', Co-CoO, Ni-NiO and Cu-Cu_2O oxygen buffers, and new data for the W-WO_2 buffer, Contrib. Mineral. Petrol. 114 (1993) 296–314.
[35] B. Fegley Jr., H. Palme, Evidence for oxidizing conditions in the solar nebula from Mo and W depletions in refractory inclusions in carbonaceous chondrites, Earth Planet. Sci. Lett. 72 (1985) 311–326.
[36] W. Schmitt, H. Palme, H. Wänke, Experimental determination of metal/silicate partition coefficients for P, Co, Ni, Cu, Ga, Ge, Mo, and W and some implications for the early evolution of the Earth, Geochim. Cosmochim. Acta 53 (1989) 173–185.
[37] M.I. Pownceby, H.St.C. O'Neill, Thermodynamic data from redox reactions at high temperatures. IV. Calibration of the Re-ReO_2 oxygen buffer from EMF and NiO+-Ni-Pd redox sensor measurements, Contrib. Mineral. Petrol. 118 (1993) 130–137.
[38] H.St.C. O'Neill, J. Nell, Gibbs free energies of formation of RuO_2, IrO_2, and OsO_2: a high-temperature electrochemical and calorimetric study, Geochim. Cosmochim. Acta 61 (1997) 5279–5293.
[39] C.-L. Chou, P.A. Baedecker, J.T. Wasson, Distribution of Ni, Ga, Ge and Ir between metal and silicate portions of H-group chondrites, Geochim. Cosmochim. Acta 37 (1973) 2159–2171.
[40] M.M. Grady, P.K. Swart, C.T. Pillinger, The variable carbon isotopic composition of type 3 ordinary chondrites, Proc. Lunar Planet. Sci. Conf. 13, J. Geophys. Res. 87 (Suppl.) (1982) A289–A296.
[41] M.M. Grady, I.P. Wright, C.T. Pillinger, A preliminary investigation into the nature of carbonaceous material in ordinary chondrites, Meteoritics 24 (1989) 147–154.
[42] G.R. Huss, R.S. Lewis, Presolar diamond, SiC, and graphite in primitive chondrites: Abundances as a function of meteorite class and petrologic type, Geochim. Cosmochim. Acta 59 (1995) 115–160.
[43] E.K. Zinner, Interstellar cloud material in meteorites, in: J.F. Kerridge, M.S. Matthews (Eds.), Meteorites and the Early Solar System, University of Arizona Press, Tucson, AZ, 1988, pp. 956–983.
[44] N.J. McNaughton, A.E. Fallick, C.T. Pillinger, Deuterium enrichments in type 3 ordinary chondrites, Proc. Lunar Planet. Sci. Conf. 13, J. Geophys. Res. 87 (Suppl.) (1982) A297–A302.
[45] D.-C. Lee, A.N. Halliday, Hf-W internal isochrons for ordinary chondrites and the initial $^{182}Hf/^{180}Hf$ of the solar system, Chem. Geol. 169 (2000) 35–43.
[46] B. Zanda, M. Bourot-Denise, C. Perron, R.H. Hewins, Origin and metamorphic redistribution of silicon, chromium, and phosphorus in the metal of chondrites, Science 265 (1994) 1846–1849.
[47] J.S. Goreva, D.S. Burnett, Phosphate control on the thorium/uranium variations in ordinary chondrites: improving solar system abundances, Meteorit. Planet. Sci. 36 (2001) 63–74.
[48] F.A. Podosek, P. Cassen, Theoretical, observational, and isotopic estimates of the lifetime of the solar nebula, Meteoritics 29 (1994) 6–25.
[49] D.S. Woolum, P. Cassen, Astronomical constraints on nebular temperatures: Implications for planetesimal formation, Meteorit. Planet. Sci. 34 (1999) 897–907.
[50] I.D. Hutcheon, R. Hutchison, Evidence from the Semarkona ordinary chondrite for ^{26}Al heating of small planets, Nature 337 (1989) 238–241.
[51] E.K. Zinner, C. Göpel, Evidence for ^{26}Al in feldspars from the H4 chondrite Ste. Marguerite, Meteoritics 27 (1992) 311–312.
[52] G.J. MacPherson, A.M. Davis, E.K. Zinner, The distribution of aluminum-26 in the early solar system – A reappraisal, Meteoritics 30 (1995) 365–386.
[53] G. Ravizza, K.K. Turekian, Application of the ^{187}Re-^{187}Os system to black shale geochronometry, Geochim. Cosmochim. Acta 53 (1989) 3257–3262.
[54] A.S. Cohen, A.L. Coe, J.M. Bartlett, C.J. Hawkesworth, Precise Re-Os ages of organic-rich mudrocks and the Os isotope composition of Jurassic seawater, Earth Planet. Sci. Lett. 167 (1999) 159–173.
[55] R.J. Walker, J.W. Morgan, M.F. Horan, Osmium-187 enrichment in some plumes: Evidence for core-mantle interaction?, Science 269 (1995) 819–822.
[56] E. Widom, S.B. Shirey, Os isotope systematics in the Azores: implications for mantle plume sources, Earth Planet. Sci. Lett. 142 (1996) 451–465.
[57] A.D. Brandon, M.D. Norman, R.J. Walker, J.W. Morgan, ^{186}Os-^{187}Os systematics of Hawaiian picrites, Earth Planet. Sci. Lett. 174 (1999) 25–42.
[58] I.S. Puchtel, M. Humayun, Platinum group elements in Kostomuksha komatiites and basalts: Implications for oceanic crust recycling and core-mantle interaction, Geochim. Cosmochim. Acta 64 (2000) 4227–4242.
[59] J.T. Wasson, X. Ouyang, J. Wang, E. Jerde, Chemical classification of iron meteorites: XI. Multi-element studies of 38 new irons and the high abundance of ungrouped irons from Antarctica, Geochim. Cosmochim. Acta 53 (1989) 735–744.
[60] E. Pernicka, J.T. Wasson, Ru, Re, Os, Pt and Au in iron meteorites, Geochim. Cosmochim. Acta 51 (1987) 1717–1726.
[61] G.W. Kallemeyn, A.E. Rubin, D. Wang, J.T. Wasson, Ordinary chondrites: bulk compositions, classification, lithophile-element fractionations, and composition-petrographic type relationships, Geochim. Cosmochim. Acta 53 (1989) 2747–2767.
[62] E. Jarosewich, Chemical analyses of meteorites: A compilation of stony and iron meteorite analyses, Meteoritics 25 (1990) 323–337.

[63] H.C. Connolly Jr., R.H. Hewins, R.D. Ash, B. Zanda, G.E. Lofgren, M. Bourot-Denise, Carbon and the formation of reduced chondrules, Nature 371 (1994) 136–139.
[64] A.E. Rubin, B. Fegley, R. Brett, Oxidation state in chondrites, in: J.F. Kerridge, M.S. Matthews (Eds.), Meteorites and the Early Solar System, University of Arizona Press, Tucson, AZ, 1988, pp. 488–511.
[65] G.R. Huss, G.J. MacPherson, G.J. Wasserburg, S.S. Russell, G. Srinivasan, Aluminum-26 in calcium-aluminum-rich inclusions and chondrules from unequilibrated ordinary chondrites, Meteorit. Planet. Sci. 36 (2001) 975–997.